IEEE Access
Multidisciplinary | Rapid Review | Open Access Journal

Received 2 December 2023, accepted 16 December 2023, date of publication 22 December 2023,
date of current version 4 January 2024.

Digital Object Identifier 10.1109/ACCESS.2023.3346173

RESEARCH ARTICLE

Design of Transcranial Magnetic Stimulation Coils With Optimized Stimulation Depth

JOSE A. VÍLCHEZ MEMBRILLA[1], MARIO F. PANTOJA[2], (Senior Member, IEEE), ANA P. VALERGA PUERTA[3], VICTOR H. SOUZA[4], AND CLEMENTE COBOS SÁNCHEZ[1]

[1]Department of Electronics, University of Cádiz, 11003 Cádiz, Spain
[2]Department of Electromagnetism, University of Granada, 18071 Granada, Spain
[3]Department of Mechanical Engineering, University of Cádiz, 11003 Cádiz, Spain
[4]Department of Neuroscience and Biomedical Engineering, School of Science, Aalto University, 02150 Espoo, Finland

Corresponding author: Clemente Cobos Sánchez (clemente.cobos@uca.es)

This work was supported by Plan Andaluz de Investigación, Desarrollo e Innovación (PAIDI 2020), Consejería de Universidad, Investigación e Innovación de la Junta de Andalucía, under Grant ProyExcel−01036.

ABSTRACT This work presents a framework to develop optimal coils of arbitrary geometry for deep transcranial magnetic stimulation (dTMS). It has been based on a continuous current density inverse boundary element method (IBEM) to generate dTMS coils with depth control and minimum power dissipation. Novel coil geometries that readily adapted to human head have been studied to provide focal stimulation in areas on both prefrontal cortex and right temporal lobe. The designed dTMS coils performance has been numerically validated in a realistic human head model and prototypes have been built for experimental evaluation. The numerical simulations indicate that the proposed dTMS coils focally stimulate the prescribed brain regions with the desired target depth. The calculated metrics demonstrate that the presented designs outperform existing dTMS coils (the stimulation depth can be increased more than 15% compared to conventional dTMS coils with similar focality). Stream function IBEM can be used to develop novel dTMS coils with improved properties for a wide range of geometries. The proposed design method opens up a possibility for exploring new coil solutions based on complex shapes to focally deliver a desired stimulation dose to relatively deep brain targets, which might allow novel and more effective brain stimulation protocols.

INDEX TERMS BEM, brain stimulation, coil design, TMS.

I. INTRODUCTION

Transcranial magnetic stimulation (TMS) is a non-invasive technique to modulate the activity of the brain, which has been successfully applied to various psychiatric and medical conditions [1], [2]. In TMS, strong current pulses are driven through a coil placed on the patient's head to induce an electric field capable of changing the neural activity. Most of the standard TMS coils used in clinical practice (such as the figure-of-eight coil) generate strong electric fields only on the cortical surface, being thus unsuitable for exciting deeper brain structures.

On the other hand, subcortical regions show promising applications to the treatment of various neurological conditions, such as bipolar depression, major depressive disorder, obsessive-compulsive disorder, epilepsy, schizophrenia, among others [3]. Deep transcranial magnetic stimulation (dTMS) coils have been proposed as alternative to traditional TMS coils [4] for depolarising neuronal populations at deeper brain structures. Some notable dTMS coil designs are [5], [6], [7], [8], [9] and the so-called H-coils [10]. The latter approach comprises a family of coils created for specific applications; such as the H1-coil and H2-coil, which have been designed to stimulate the prefrontal cortex (PFC) [11], [12] or the H12-coil tailored for stimulating the right temporal lobe (RTL) [13].

The associate editor coordinating the review of this manuscript and approving it for publication was Vincent Chen.

All the previously mentioned approaches [5], [6], [7], [8], [9], [10], [11], [12], [13] are based on basic coil elements with well-known magnetic profiles which are combined empirically or by simple heuristics to drive electromagnetic fields deeper into the brain, providing thus suboptimal solutions to dTMS coil design problem. Moreover, in this type of designs, the improvement of the stimulation depth is frequently achieved by employing coils with larger dimensions, resulting in the need of higher currents to create comparable stimulation to that one found in conventional TMS.

These facts highlight that the advancement of dTMS as an effective tool in neuroscience would highly benefit from the development of a design framework capable of producing optimal coils with geometries better matched to the human head and controlling the spatial characteristic of the induced E-field, along with other physical features, such as resistance or inductance, in the design process.

Recently, new TMS coil design techniques based on continuous current density models have arisen [14], [15], producing spherical and flat TMS transducers with optimal trade-off between depth and focality of the induced electric field [16], [17]. Amongst this group of continuous current density methods, those techniques incorporating the stream function of a quasi-static surface current density within an inverse boundary element method (IBEM) have been especially successful. They have allowed a wide variety of coil geometries subjected to different performance requirements, such as minimum power dissipation and minimum inductance [18], [19], [20], [21], [22]. Additionally, stream function IBEM permits to consider the spatial characteristics of the stimulation in the design process [19], [22], whereas its potentialities to generate optimal coil solutions with prescribed penetration for dTMS have not been studied yet.

In this work, we propose the use of a stream function IBEM to produce minimum power dissipation dTMS coils with depth control and based on geometries tailored to the human head. A new head-shaped geometry would bring the transducer closer to the target region, improving the stimulation efficiency on the desired deep brain structures. The capabilities of the proposed approach are illustrated by designing three specific TMS coils using different new shapes closely matching the human head to target deep areas in both PFC and right temporal region, where there exist potential treatments to different neurological conditions [12], [13]. The performance of each dTMS coil has been numerically evaluated using finite element method simulations [23] in a realistic human head model [24]; whereas experimental characterisation has also been achieved by building and testing two prototypes of the designed coils.

II. METHODOLOGY

A. STREAM FUNCTION IBEM

The following is a brief outline of the stream function IBEM; for a complete description of the method, we refer to the original works [25], [26]. In a stream function IBEM the continuous current distribution under search is found through the solution of an optimization problem formulated in terms of the stream function. The numerical model of the current density is achieved by meshing the coil conducting surface into triangular elements and N nodes. It can be expressed as:

$$J(r,\psi) \approx \sum_{n=1}^{N} \psi_n \, \boldsymbol{J}^n(r), \quad r \in S, \tag{1}$$

where $\psi = (\psi_n, \psi_n, \ldots \psi_n)$ is vector containing the nodal values of the stream function and $\boldsymbol{J}^n(r)$ is the current element associated to the n^{th}-node [26]. In a stream function IBEM, ψ is the optimization variable.

By using the current density model in (1), the discretized version of the different physical magnitudes involved in the design problem can be obtained, for instance:

- The x_i component of the electric field induced by the coil:

$$E_{x_i}(r,\psi) \approx \sum_{n=1}^{N} \psi_n e^n_{x_i}(r), \tag{2}$$

  where $e^n_{x_i}$ is the electric field vector produced by a unit stream function at the *nth*-node [19], with $x_i = x, y, z$.
- The resistive power dissipation by the coil:

$$P(\psi) \approx \sum_{n=1}^{N}\sum_{m=1}^{N} \psi_n \psi_m R_{nm}, \tag{3}$$

  where R is the resistance matrix [26].

These properties allow one to construct the equations used to pose the coil design problem as a convex optimisation, of which the solution is the optimal stream function. The final wire arrangement that approximates the current density is obtained by connecting in series the equally-spaced contour lines of the stream function [27].

B. METRICS DEFINITION

In order to evaluate the spatial characteristics of the stimulation, the following metrics have been used. For the sake of comparison to the existing TMS coils, these parameters have been computed in both realistic and spherical head models.

• SUPRATHRESHOLD VOLUME, $V_{1/2}$

It is the region in which the electric field strength is above the stimulation threshold E_{th}. It can be defined as in [16]:

$$V_{1/2} = \int_{Brain} B(\|E(r)\| - E_{th}) d^3 r, \tag{4}$$

where $E(r)$ is the electric field at a given point $\mathbf{r}$ in the brain and $B(x)$ is the step function.

$$B(x) = \begin{cases} 1, & x \geq 0 \\ 0, & x < 0 \end{cases} \tag{5}$$

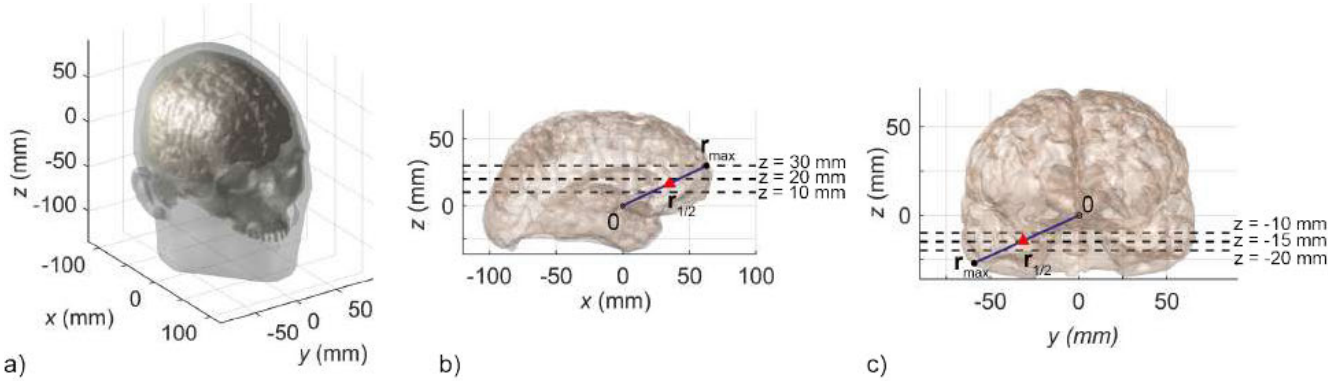

FIGURE 1. a) The three-compartment head model (scalp, skull and brain) obtained from the Virtual Family Project [24]. Positioning of the brain center and schematic representation of the depth definition used for b) PFC and c) RTL stimulation design problems respectively.

Hereinafter it has been assumed that $E_{th} = 50$ V/m and the maximum electric field strength acceptable is twice the threshold value [16]. In practice, this maximum electric field value will be achieved by adjusting the current amplitudes through the coils, as will be shown in Section III-B.

• MAXIMUM DEPTH OF STIMULATION, $D_{1/2}$

Also referred to as penetration, it is the greatest distance along a given direction where the stimulus is over 50% of the maximum [16]. In this work, two points in the brain (r_{max} and $r_{1/2}$) are chosen to describe the line in which $d_{1/2}$ is computed. In the particular case of a spherical head model (where the cortex is taken as a sphere of 7-cm radius [7]), the depth of the stimulation $d_{1/2}$ becomes the radial distance from the cortical surface to the deepest point where the E-field is equal to the threshold.

• FOCALITY, $S_{1/2}$

It represents the spread of the stimulation and quantifies the average transverse surface area of the suprathreshold region [16]. Focality can be expressed as:

$$S_{1/2} = \frac{V_{1/2}}{d_{1/2}}. \tag{6}$$

C. OPTIMISATION PROBLEM

In order to design TMS coils with the desired stimulation depth using the stream function IBEM, the following optimisation problem is proposed:

$$\begin{cases} \text{mín} P(\psi) \\ \text{subject to} \\ E(r_{max}) \cdot \hat{t} = 2E_{th} \\ E(r_{1/2}) \cdot \hat{t} = E_{th} \end{cases} \tag{7}$$

where ψ is a vector containing the nodal values of the stream function (the optimization variables), r_{max} is the point at the cortical surface where the E-field strength reaches its maximum value, $r_{1/2}$ is the point at the targeted depth in the desired brain region and vector $\hat{t}$ describes the preferential direction of the stimulation [16].

Furthermore, all coil design problems in this work can be formulated as the optimisation in 7. It can be analytically tackled by using elements from theory of Banach Spaces and Operator Theory [19], [28], which allow to obtain truly optimal solutions for this kind of problems.

D. HUMAN HEAD MODEL

An anatomically realistic human head model has been used to study the stimulation produced by the different TMS coils proposed here. It was developed for the Virtual Family Project [24] and consists of magnetic resonance imagining (MRI) data of a 34 years old male with a height of 1.77 m weighting 70.3 kg. The heterogeneity of the electric properties of the human head has been taken into account with a three-compartment scalp-skull-brain model of conductivities 0.465, 0.01 and 0.276 S/m respectively [16]. Moreover the skin, skull and brain surfaces were meshed into 4740, 137126, and 93314 triangular elements respectively, as shown in Fig. 1.

E. COIL DESIGN EXAMPLES

The objective of this work involves the design of application-tailored coils for dTMS with controlled stimulation depth and minimum power dissipation. To this end our designs are based on the following considerations:

1) The focality and efficiency of the stimulation strongly depend on the distance between the transducer and the target region. Consequently, the coil geometries considered in this work have been chosen to fit properly the corresponding part of the scalp, bringing the TMS coil closer to the target region.
2) TMS coil design typically frequently results in quite dense coil patterns. In order to ameliorate this problem, we have considered each coil surface with a defined thickness, allowing wire distribution in both connected sides.
3) For all designs, we have prescribed a penetration of 3 cm along a given direction in a homogeneous single domain brain model surrounded by air.

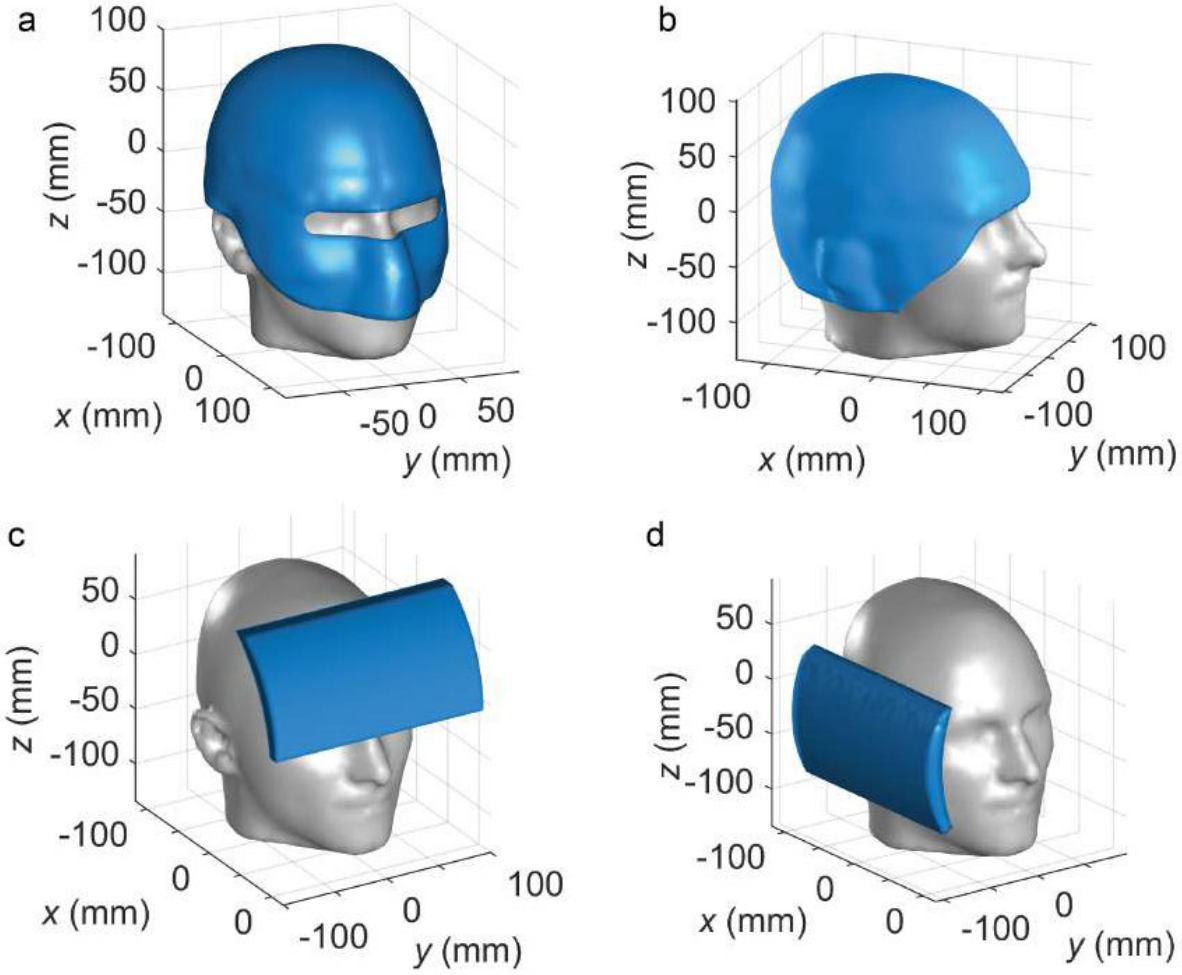

FIGURE 2. Schematic diagrams showing the geometry of a) the helmet-like dTMS Coil 1, b) geometry of the 'cap-like' dTMS Coil 2, c) and d) the curved hexahedral dTMS Coil 3, along with the human head model used as reference. The two positions of the conducting surface of dTMS Coil 3 illustrate the coil placements considered for activation of the PFC and RTL respectively.

TABLE 1. Stimulation spatial conditions used in the designs.

	dTMS Coil 1	dTMS Coil 2	dTMS Coil 3
$\mathbf{r}_{max}$ (mm)	$(63{,}2, 0, 30{,}1)$	$(1{,}3, -59{,}0, -27{,}0)$	$(63{,}2, 0, 30{,}1)$
$\mathbf{r}_{1/2}$ (mm)	$(35{,}8, 0, 17{,}0)$	$(0{,}7, -31{,}6, -14{,}4)$	$(35{,}8, 0, 17{,}0)$
$\hat{\mathbf{t}}$	$\hat{\mathbf{z}}$	$\hat{\mathbf{y}}$	$\hat{\mathbf{z}}$

4) For each design problem, the number of stream function contour levels (and equivalently the number of coil turns) was maximised whilst ensuring that the minimum wire spacing remained above 0.75 mm, considering a thickness of 1 mm for all wires.

These criteria have been applied to produce three dTMS coils based on different geometries (Fig. 2). The line employed to set the stimulation depth is shown in Figs. 1 b) and c) for the case of PFC stimulation RTL stimulation respectively, whereas Table 1 shows the corresponding values of r_{max}, $r_{1/2}$ and $\hat{t}$ for the three dTMS coils [16].

1) DTMS COIL 1

The first coil geometry is depicted in Fig. 2a), consisting of a helmet-like shape of 4-mm thickness targeted to PFC. This geometry has been derived from the human head model scalp surface in Fig. 1, where a 'window' (from which wires are excluded) has been incorporated to reduce potential risks of ophthalmic adverse events and to allow visual interaction with the subject. The inclusion of the window may also significantly ameliorate the claustrophobia perception in many subjects.

2) DTMS COIL 2

The second coil geometry shown in Fig. 2b) was designed to target the RTL. This design is a 'cap-like' surface of 4-mm thickness that has been created from the human head model in Fig. 1. The motivation of using this geometry relies on its readily adaptation to most of the (adult) head shapes.

TABLE 2. Performance parameters for the designed TMS coils. Simulated values of the inductance L and resistance R obtained with COMSOL [23]. In square brackets are the measured values L and R of the prototypes. $d_{1/2}$ is the maximum depth of stimulation, $V_{1/2}$ suprathreshold volume and $S_{1/2}$ the focality computed in a realistic three-compartment human head model. In square brackets are the computed values in a spherical head model [7]. $d^B_{1/2}$ is the penetration calculated in a homogeneous single domain brain model surrounded by air.

	dTMS coil 1	dTMS coil 2	dTMS coil 3 PFC	dTMS coil 3 RTL
L (μH)	91 [102]	100 [108]	19 [-]	19 [-]
R (mΩ)	271 [354]	278 [359]	109 [-]	109 [-]
$d_{1/2}$ (cm)	2.7 [2.5]	2.2 [2.4]	1.7 [2.0]	1.6 [2.0]
$S_{1/2}$ (cm^2)	95 [129]	100 [52]	17 [29]	30 [29]
$V_{1/2}$ (cm^3)	255 [342]	217 [206]	29 [58]	47 [58]
$d^B_{1/2}$ (cm)	3.0	2.8	2.6	2.8

3) DTMS COIL 3

The third design example involved generating a multi-purpose dTMS coil that can be used to target either PFC or RTL. Thus, a curved hexahedral coil shape of 4-mm thickness with an original size of 20 cm × 9.5 cm has been subsequently curved in order to fit both forehead and scalp area around the temple, as depicted in Figs. 2c) and 2d), respectively, where the relative positions employed for dTMS Coil 3 surface with respect to the head are shown.

F. NUMERICAL SIMULATIONS

Numerical validation of the designed dTMS coils was performed using the COMSOL Multiphysics software [23]. Three dimensional models of the coils were created and the AC/DC Module was employed to evaluate the stimulation produced in the human head model (section II-D) and to compute the spatial characteristics of the stimulation (section II-B). The resistance and inductance of each dTMS coil were also computed with COMSOL.

G. PROTOTYPE COIL CONSTRUCTION

In order to experimentally evaluate the proposed approach, prototypes of the designed dTMS coils were manufactured and tested. They were built using a 3D printer with fused deposition modelling technology and polylactic acid (PLA) as material. The printhead has a diameter of 0.4 mm, and a layer height of 0.2 mm was used to minimize geometric deviations of complex surfaces. Grooves were printed on both sides of each mold, where the depth and width of the slot were chosen to be 2 mm, in which copper wire of a 1 mm thickness was inserted and glued with epoxy. After manufacture, the inductance and resistance of all the prototype coils were measured using an LCR-meter and a digital multimeter respectively. In this regard, it is worth noting that the coil prototypes were built in order to verify their manufacturability and physical properties, and they are not intended to be tested for stimulation on evaluated on human subjects.

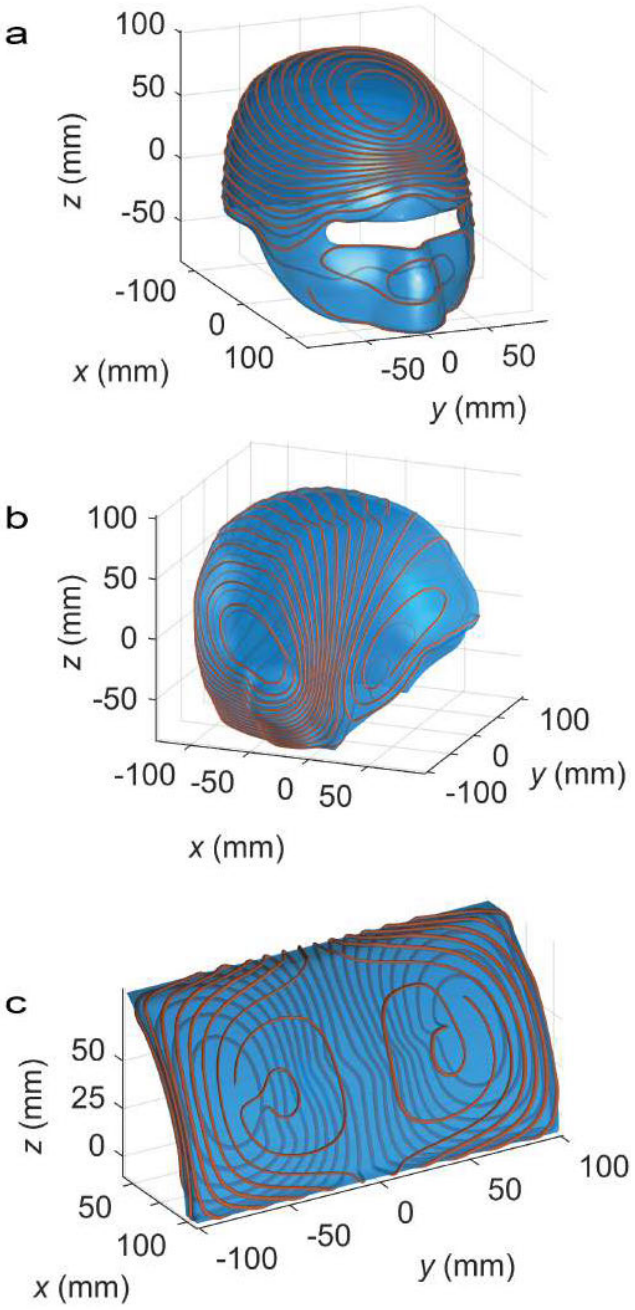

FIGURE 3. Wire-path for a) dTMS Coil 1, b) dTMS Coil 2 and c) dTMS Coil 3.

III. RESULTS

A. DTMS COIL DESIGNS

The winding pattern solutions of the dTMS coil design problems presented in section II-E are shown. They have been produced by firstly equally-spaced contouring the stream function, and secondly connecting in series the resulting

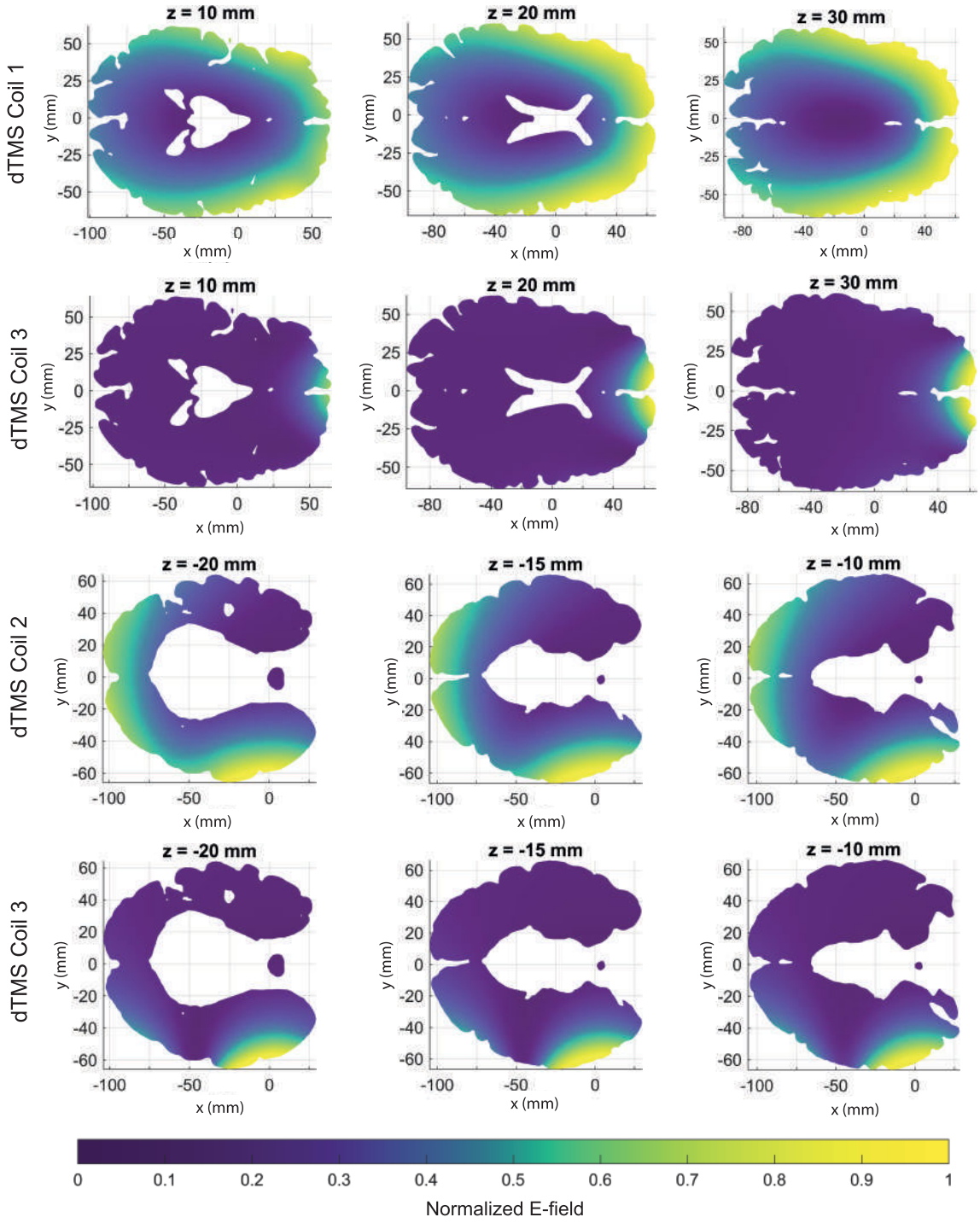

FIGURE 4. Normalised electric field distributions for dTMS Coils 1, 2, and 3 on different axial slices from the realistic brain model. The first and second rows show the corresponding E-field due to the dTMS Coils 1 and 3 on the $xy-$planes at $z = 10$, 20 and 30 mm (Fig. 1b) respectively. The third and fourth rows show the corresponding E-field due to the dTMS Coils 2 and 3 on the $xy-$planes at $z = -20$, -15 and -10 mm (Fig. 1c) respectively. E-field distributions were normalised for clarity in visually evaluating the spatial characteristics.

unconnected contour lines. The performance properties of the dTMS coils are listed in Table 2.

Fig. 3a) illustrates the coil layout for the dTMS Coil 1. It can be seen that wires are excluded from the window area, which both may facilitate visual interaction with the subject and allay patient claustrophobia concerns. Moreover, higher density of winding turns occurs over the frontal region. Analogously, Fig. 3b) depicts the wire path obtained for the dTMS Coil 2 design. In this case, the coil has four independent lobes of wire, two in each side of the cap shaped

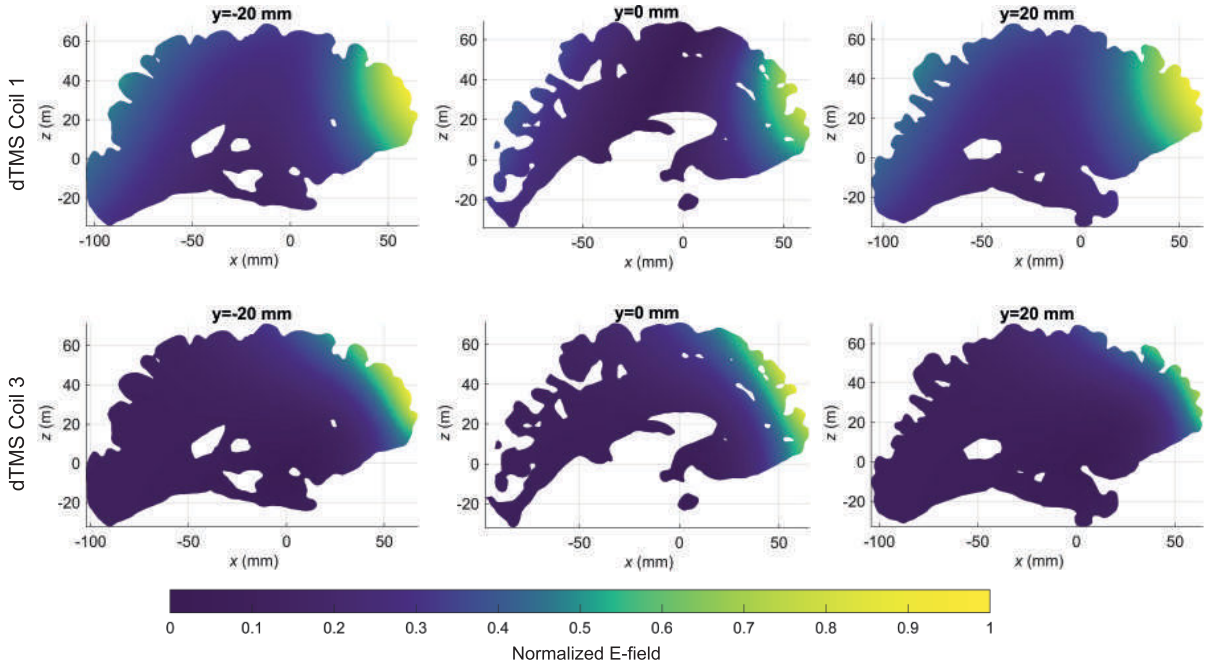

FIGURE 5. Normalised electric field distributions for dTMS Coils 1 and 3 on different sagittal slices from the realistic brain model. The first and second rows show the corresponding E-field due to the dTMS Coils 1 and 3 on the $xz-$planes at $y = -20$, 0 and 20 mm (Fig. 1b) respectively. E-field distributions were normalised for clarity in visually evaluating the spatial characteristics.

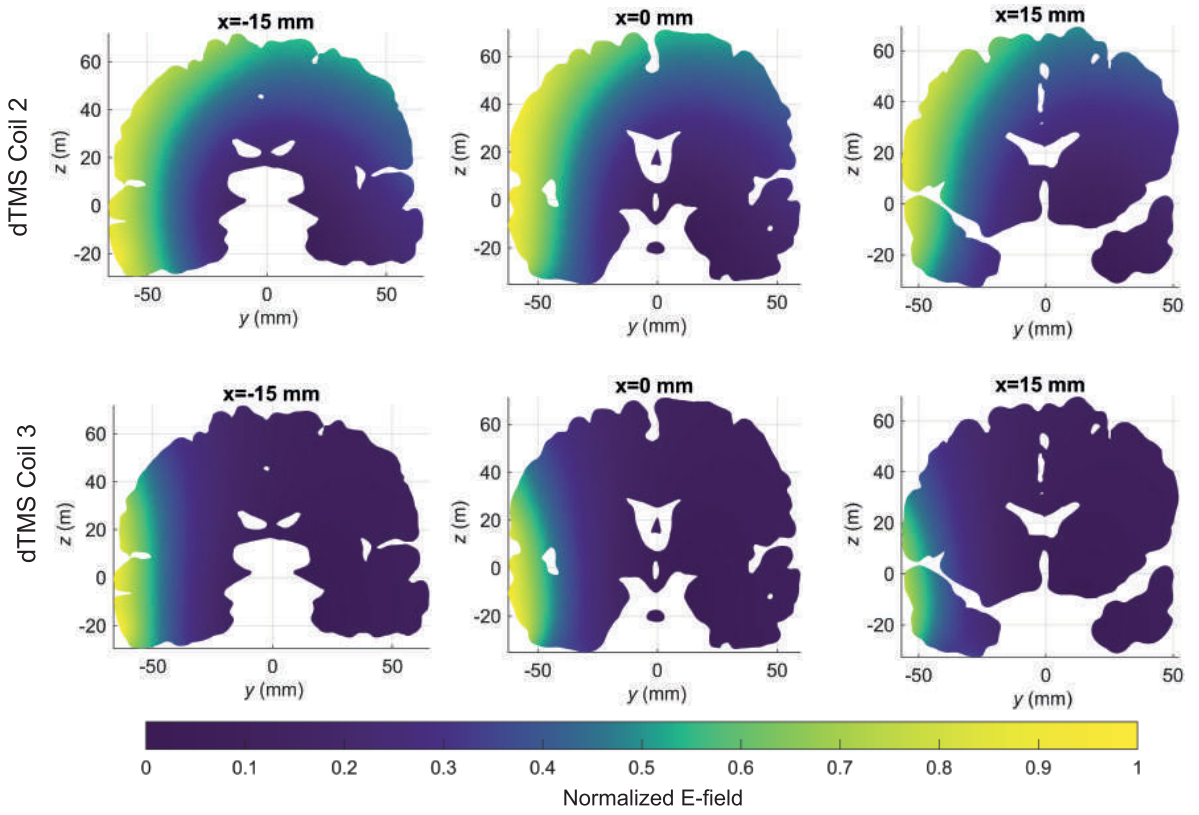

FIGURE 6. Normalised electric field distributions for dTMS Coils 2 and 3 on different coronal slices from the realistic brain model. The first and second rows show the corresponding E-field due to the dTMS Coils 2 and 3 on the $yz-$planes at $x = -15$, 0 and 15 mm (Fig. 1b) respectively. E-field distributions were normalised for clarity in visually evaluating the spatial characteristics.

surface. As expected, a higher density of winding turns occurs over the target region. Finally, the coil layout corresponding to the solution dTMS Coil 3 coil design problem is shown in Fig. 3c), where it can be again noted that the use of both connected sides of the coil former surface makes the best possible use of the space closest to the region of stimulation. There is a high concentration of wire elements at the inner side of the coil surface, while the outer side provides a return path for the wires.

B. COMPUTATIONAL EVALUATION

Assuming a sinusoidal variation ($f = 3$ kHz [16]) these are the current amplitudes in order to achieve a maximum electric field strength of 100 V/m in the cortex: dTMS Coil 1 (0.81 kA); dTMS Coil 2 (0.89 kA) and dTMS Coil 3 (2.25 kA for PFC and 3.10 kA for RTL).

1) PREFRONTAL CORTEX

As it can be seen in Figs. 4 and 5, dTMS Coil 1 induces an E-field on a large volume in the PFC providing bilateral stimulation of the dorsolateral and ventrolateral regions, and even an undesired activation of the temporal regions. On the other hand, dTMS Coil 3 when placed over the frontal region of the realistic head model, as shown in Fig. 2c, generates a more focal stimulation in medial prefrontal regions but with reduced penetration: its suprathreshold volume in a realistic head model is the 11% of the one produced by dTMS Coil 1, nonetheless dTMS Coil 3 depth is approximately 1 cm less than the penetration of its counterpart, as it can be seen in Table 2. This fact is also confirmed when evaluating the simulated metrics of each coil in a spherical head model.

2) RIGHT TEMPORAL LOBE

As it can be seen in the third and fourth row of Fig. 4, both dTMS Coil 2 and 3 surpass the neuronal activation threshold in RTL structures, where dTMS Coil 2 stimulates a larger volume in this part of the brain. This behaviour is also appreciated when evaluating the E-field on different coronal slices (Fig. 6), and it is consistent with the metrics in Table 2 where it can be seen that the suprathreshold volume of dTMS Coil 3 in a realistic head model is the 22% of the one produced by dTMS Coil 2. Moreover, the stimulation depth of dTMS Coil 3 in a realistic head model is 0.6 cm less than the one found for dTMS Coil 2. It is also worth noting that although stimulation induced by the cap-like coil is mainly over the RTL, there is an undesired activation in the occipital lobe (Fig. 4).

3) ATTENUATION IN DEPTH

Fig. 7 shows the normalised electric field induced as a function of distance from r_{max} along the corresponding depth definition line in the brain for each coil. The comparison between the dTMS coils confirms a greater depth penetration for dTMS Coil 1 and dTMS Coil 2, whereas the stimulation of dTMS Coil 3 decay more rapidly with distance from the scalp.

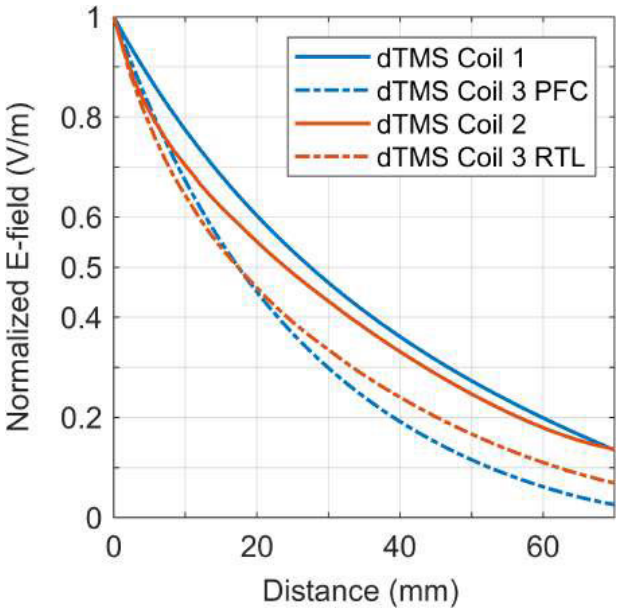

FIGURE 7. Normalised electric field induced as a function of distance along the corresponding depth definition line in the brain.

C. PROTOTYPES

Experimental characterisation of the proposed approach was performed by building and testing prototypes of two coils presented in this paper, namely dTMS Coil 1 and 2 in Figs. 3 a) and b), respectively. The corresponding manufactured prototypes of these transducer coils are shown in Figs. 8a) and b) respectively, whereas the measured inductance and resistance values can be found in square brackets in Table 2. It is worth noting that the measured values of L differ from those obtained with COMSOL by 10% for dTMS Coil 1 and 7% for dTMS Coil 2. Measured and numerically calculated values of R differ about 24% in both cases.

IV. DISCUSSION

By using a stream function IBEM, we presented optimal dTMS coils with shapes tailored to the human head and subjected to different performance constraints. The results obtained confirm two main advantages of the proposed design technique that are discussed below.

A. GEOMETRY-INDEPENDENT METHOD

Stream function IBEM allows the inclusion of complex geometries in the design process. We used this feature to:

1) BRING THE COIL CLOSER TO THE TARGET REGION

In order to generate the most efficient stimulation, we have considered novel geometries that permit placing the current carrying surfaces as close to the target region as possible. The shapes of dTMS Coil 1 and 2 were also chosen to accommodate most of adults head sizes, nonetheless there may exist a variable gap between the scalp and each TMS coil. For instance, it was found that the minimum spacing between the coil (considering the wires thickness) and the surface of the realistic head model was of the order of 3-5 mm in all the

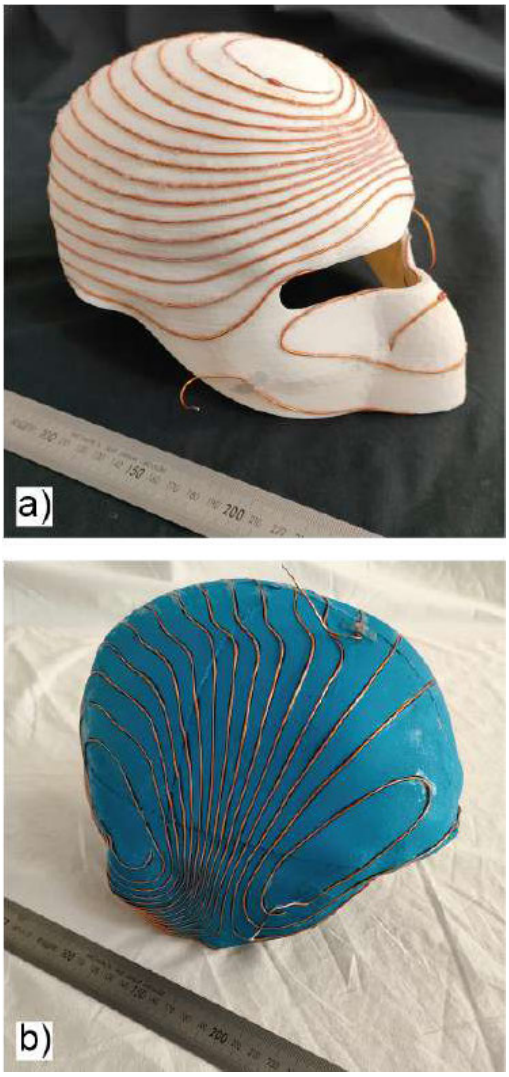

FIGURE 8. Photographs of the manufactured prototype for a) dTMS Coil 1 and b) dTMS Coil 2. All coils were wound with copper wire of 1-mm thickness inserted in grooves on a 3D-printed plastic former.

designs presented here. In that sense, it would be interesting to consider the production of the TMS coils proposed in multiple sizes to better adapt the different range of head sizes.

2) INCLUDE A WINDOW IN THE DESIGN OF DTMS COIL 1

This strategy may ameliorate significantly the claustrophobia perception and allow visual interaction with the subject. It is worth noting that one disadvantageous consequence of incorporating the window in the design of dTMS Coil 1 coil surface is the reduction of the performance: for the same depth (2.7 cm) in a realistic head model the coil geometry shown in Fig. 2 without the window would allow the design of a coil with less resistance (301 mΩ) and improved focality (89 cm^2).

3) CONSIDER COIL SURFACE WITH A DEFINED THICKNESS

In general, TMS coil designs exhibit areas of high winding density (especially over the region of stimulation), this may become an important hindrance even leading to unpractical designs [16], specially in coils that are constructed from finite sized wire where there is a minimum wire separation that can be built [22]. In this paper, this problem has been ameliorated by allowing the current flow between both connected sides of a given surface with defined thickness, which may also have some other potential benefits, including improved thermal behaviour [19].

B. INCLUSION OF PERFORMANCE REQUIREMENTS

Stream function IBEM permits the inclusion of many constraints and properties in the design process [19] and [20], which may also be used to satisfy other functional and technical requirements needed for dTMS.

1) RESISTANCE AND INDUCTANCE

dTMS coils with reduced inductance and controlled depth can be directly produced by substituting minimum power dissipation condition in equation 7 by a minimum magnetic stored energy constraint, which would pose an equivalent optimisation problem due to the similar nature of these two magnitudes [19].

It is also worth noting that the simulated and measured values of the resistance in Table 2 are higher than those found in conventional TMS coils, which may be justified, in part by the large number of turns of wire used in the proposed IBEM coils. Although the used of 1.0 mm diameter copper wire is frequently use for TMS coil design [14], [18], the resistance of the prototypes can be significantly reduced by using thicker wires (which can be achieved by reducing the imposed minimum wire spacing) or decreasing the number of turns of wire.

2) SPATIAL CHARACTERISTICS OF THE STIMULATION

A penetration of 3 cm in a homogeneous brain model surrounded by air was prescribed for all designs. A more relevant characterization of the penetration could be produced by imposing a desired value of $d_{1/2}$ in the realistic three-compartment head model. This could be achieved using stream function IBEM, as it also permits the modelling of the E-field in heterogeneous conducting systems [19]. Nonetheless, the use of more biologically complex models remarkably increases the computational burden in the solution of (7). In this regard, as it can be seen in Table 2, the values of $d_{1/2}$ computed in a realistic head model are lower than 3 cm for all coils. This reduction was expected, since there are additional E-field contributions due to accumulation of charges in the boundaries between regions of different conductivity that reduce the penetration of the stimulation. Moreover the penetration calculated in a homogeneous single-domain brain model surrounded by air, $d^B_{1/2}$, for dTMS Coil 2 and dTMS Coil 3 is less than 3 cm, which may be partially explained due to the series connection that must be performed in the coil.

Nonetheless, it is worth stressing that the dTMS coils designed successfully induce strong E-fields in deep areas in both PFC and right temporal region, remarkably outperforming state-of-the-art dTMS coils [4].

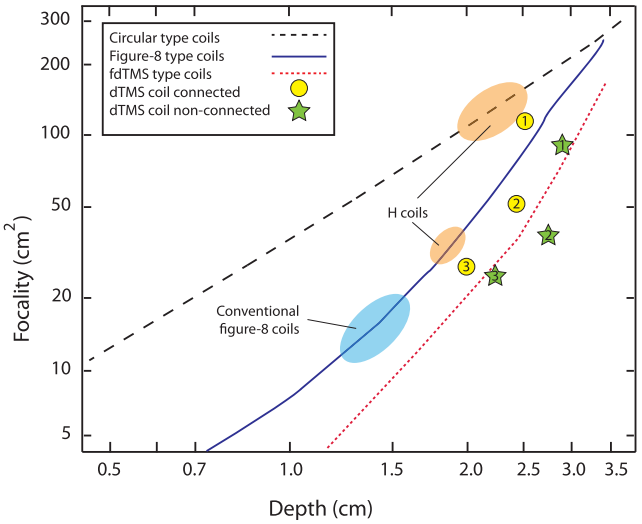

FIGURE 9. Focality as a function of the maximum depth of stimulation of the existing coils, this plot is a modified version from those found in [7], [16] (see these references for more information of the specific coils). Green star and yellow circle markers denote dTMS coil designs proposed in this work before and after connecting in series, respectively. The metrics before connecting in series for a spherical head model are: dTMS Coil 1 ($d_{1/2}$= 2.7 cm and $s_{1/2}$= 41 cm^2); dTMS Coil 2 ($d_{1/2}$= 2.7 cm and $s_{1/2}$= 41 cm^2); dTMS Coil 3 ($d_{1/2}$= 2.2 cm and $s_{1/2}$= 23 cm^2).

For instance, if we consider a spherical head model, dTMS Coil 2 provides a penetration approximately 4 mm larger than conventional dTMS coils with similar focality, whereas dTMS coil 3 offers more than a 20% focality reduction compared to existing TMS coils with equivalent depth [7], as it can be seen in Fig. 9 where the yellow circle denotes the dTMS coils designed in this work.

Furthermore, in order to make a fair comparison to other state of art approaches, the dTMS coil solutions proposed in this work before connecting in series have been included in Fig. 9 with green stars markers. It can be seen that the dTMS Coil 2 and dTMS Coil 3 offer an improved trade-off between depth and focality compared to designs proposed in [16]. However, dTMS Coil 1 design (star 1 in Fig. 9) is above the red dot line from [16], which is justified by the inclusion of the window.

C. LIMITATIONS AND FUTURE WORK

One of the main limitations of the presented approach is the undesired stimulation of non-target brain regions, which degrades TMS precision. Facial nerve and muscle stimulation may be also concerns for suprathreshold TMS.

Future work will include the application of the stream function IBEM to obtain an overall view of the achievable trade-off between the penetration and focality of the induced E-field. In addition, the proposed design framework may have potential applications to other forms of TMS, such as low field magnetic stimulation where efficient coils that conform to the head shape are required [15], [29], [30].

V. CONCLUSION

We presented a design framework for creating dedicated dTMS coils wound on arbitrarily shaped surfaces allowing the inclusion of different performance requirements, such as penetration depth and power dissipation. Three dTMS coils have been designed using novel geometries that offer much sparser wire spacing and bring the coil closer to the target region, thus improving the stimulation efficiency. They provide an optimal compromise between depth and power dissipation, outperforming current state of the art dTMS design approaches. The proposed coil design method opens up a possibility for exploring new coil solutions of complex shapes to focally stimulate deeper brain targets, which might contribute to the emergence of novel clinical applications.

REFERENCES

[1] E. Wasserman, C. M. Epstein, and U. Ziemann, *The Oxford Handbook of Transcranial Stimulation*. Oxford, U.K.: Oxford Univ. Press, 2011.

[2] S. Rossi et al., "Safety and recommendations for TMS use in healthy subjects and patient populations, with updates on training, ethical and regulatory issues: Expert guidelines," *Clin. Neurophysiol.*, vol. 132, no. 1, pp. 269–306, Jan. 2021.

[3] F. S. Bersani, A. Minichino, P. G. Enticott, L. Mazzarini, N. Khan, G. Antonacci, R. N. Raccah, M. Salviati, R. D. Chiaie, G. Bersani, P. B. Fitzgerald, and M. Biondi, "Deep transcranial magnetic stimulation as a treatment for psychiatric disorders: A comprehensive review," *Eur. Psychiatry*, vol. 28, no. 1, pp. 30–39, Jan. 2013.

[4] Z.-D. Deng, S. H. Lisanby, and A. V. Peterchev, "Coil design considerations for deep transcranial magnetic stimulation," *Clin. Neurophysiol.*, vol. 125, no. 6, pp. 1202–1212, Jun. 2014.

[5] P. M. Kreuzer, J. Downar, D. de Ridder, J. Schwarzbach, M. Schecklmann, and B. Langguth, "A comprehensive review of dorsomedial prefrontal cortex rTMS utilizing a double cone coil," *Neuromodulation, Technol. Neural Interface*, vol. 22, no. 8, pp. 851–866, Dec. 2019.

[6] K. R. Davey and M. Riehl, "Suppressing the surface field during transcranial magnetic stimulation," *IEEE Trans. Biomed. Eng.*, vol. 53, no. 2, pp. 190–194, Feb. 2006.

[7] Z.-D. Deng, S. H. Lisanby, and A. V. Peterchev, "Electric field depth—Focality tradeoff in transcranial magnetic stimulation: Simulation comparison of 50 coil designs," *Brain Stimulation*, vol. 6, no. 1, pp. 1–13, Jan. 2013.

[8] M. Lu and S. Ueno, "Computational study toward deep transcranial magnetic stimulation using coaxial circular coils," *IEEE Trans. Biomed. Eng.*, vol. 62, no. 12, pp. 2911–2919, Dec. 2015.

[9] L. Gomez, F. Cajko, L. Hernandez-Garcia, A. Grbic, and E. Michielssen, "Numerical analysis and design of single-source multicoil TMS for deep and focused brain stimulation," *IEEE Trans. Biomed. Eng.*, vol. 60, no. 10, pp. 2771–2782, Oct. 2013.

[10] Y. Roth, F. Padberg, and A. Zangen, "Transcranial magnetic stimulation of deep brain regions: Principles and methods," in *Transcranial Brain Stimulation for Treatment of Psychiatric Disorders*. Basel, Switzerland: S. Karger AG, Mar. 2007, doi: 10.1159/000101039.

[11] Y. Roth, A. Amir, Y. Levkovitz, and A. Zangen, "Three-dimensional distribution of the electric field induced in the brain by transcranial magnetic stimulation using figure-8 and deep H-coils," *J. Clin. Neurophysiol.*, vol. 24, no. 1, pp. 31–38, 2007.

[12] Y. Levkovitz, E. V. Harel, Y. Roth, Y. Braw, D. Most, L. N. Katz, A. Sheer, R. Gersner, and A. Zangen, "Deep transcranial magnetic stimulation over the prefrontal cortex: Evaluation of antidepressant and cognitive effects in depressive patients," *Brain Stimulation*, vol. 2, no. 4, pp. 188–200, Oct. 2009.

[13] R. Gersner, L. Oberman, M. J. Sanchez, N. Chiriboga, H. L. Kaye, A. Pascual-Leone, M. Libenson, Y. Roth, A. Zangen, and A. Rotenberg, "H-coil repetitive transcranial magnetic stimulation for treatment of temporal lobe epilepsy: A case report," *Epilepsy Behav. Case Rep.*, vol. 5, pp. 52–56, Mar. 2016.

[14] L. M. Koponen, J. O. Nieminen, and R. J. Ilmoniemi, "Minimum-energy coils for transcranial magnetic stimulation: Application to focal stimulation," *Brain Stimulation*, vol. 8, no. 1, pp. 124–134, Jan. 2015.

[15] B. Wang, M. R. Shen, Z.-D. Deng, J. E. Smith, J. J. Tharayil, C. J. Gurrey, L. J. Gomez, and A. V. Peterchev, "Redesigning existing transcranial magnetic stimulation coils to reduce energy: Application to low field magnetic stimulation," *J. Neural Eng.*, vol. 15, no. 3, Apr. 2018, Art. no. 036022.
[16] L. J. Gomez, S. M. Goetz, and A. V. Peterchev, "Design of transcranial magnetic stimulation coils with optimal trade-off between depth, focality, and energy," *J. Neural Eng.*, vol. 15, no. 4, Aug. 2018, Art. no. 046033.
[17] S. Nurmi, J. Karttunen, V. H. Souza, R. J. Ilmoniemi, and J. O. Nieminen, "Trade-off between stimulation focality and the number of coils in multi-locus transcranial magnetic stimulation," *J. Neural Eng.*, vol. 18, no. 6, Nov. 2021, Art. no. 066003.
[18] C. C. Sánchez, J. M. G. Rodriguez, Á. Q. Olozábal, and D. Blanco-Navarro, "Novel TMS coils designed using an inverse boundary element method," *Phys. Med. Biol.*, vol. 62, no. 1, pp. 73–90, Jan. 2017.
[19] C. C. Sánchez, F. J. Garcia-Pacheco, J. M. G. Rodriguez, and J. R. Hill, "An inverse boundary element method computational framework for designing optimal TMS coils," *Eng. Anal. Boundary Elements*, vol. 88, pp. 156–169, Mar. 2018.
[20] C. C. Sánchez, F. J. Garcia-Pacheco, J. M. Guerrero-Rodriguez, and L. Garcia-Barrachina, "Solving an IBEM with supporting vector analysis to design quiet TMS coils," *Eng. Anal. Boundary Elements*, vol. 117, pp. 1–12, Aug. 2020.
[21] L. M. Koponen, J. O. Nieminen, T. P. Mutanen, M. Stenroos, and R. J. Ilmoniemi, "Coil optimisation for transcranial magnetic stimulation in realistic head geometry," *Brain Stimulation*, vol. 10, no. 4, pp. 795–805, Jul. 2017.
[22] I. J. Rissanen, V. H. Souza, J. O. Nieminen, L. M. Koponen, and R. J. Ilmoniemi, "Advanced pipeline for designing multi-locus TMS coils with current density constraints," *IEEE Trans. Biomed. Eng.*, vol. 70, no. 7, pp. 2025–2034, 2023, doi: 10.1109/TBME.2023.3234119.
[23] *COMSOL Multiphysics*. Version 5.6. Comsol AB, Stockholm, Sweden, 2021. [Online]. Available: https://www.comsol.es
[24] M.-C. Gosselin, E. Neufeld, H. Moser, E. Huber, S. Farcito, L. Gerber, M. Jedensjö, I. Hilber, F. D. Gennaro, B. Lloyd, E. Cherubini, D. Szczerba, W. Kainz, and N. Kuster, "Development of a new generation of high-resolution anatomical models for medical device evaluation: The virtual Population 3.0," *Phys. Med. Biol.*, vol. 59, no. 18, pp. 5287–5303, Aug. 2014.
[25] S. Pissanetzky, "Minimum energy MRI gradient coils of general geometry," *Meas. Sci. Technol.*, vol. 3, no. 7, pp. 667–673, Jul. 1992.
[26] M. Poole and R. Bowtell, "Novel gradient coils designed using a boundary element method," *Concepts Magn. Reson. B, Magn. Reson. Eng.*, vol. 31, no. 3, pp. 162–175, Aug. 2007.
[27] M. A. Brideson, L. K. Forbes, and S. Crozier, "Determining complicated winding patterns for shim coils using stream functions and the target-field method," *Concepts Magn. Reson.*, vol. 14, no. 1, pp. 9–18, Jan. 2002.
[28] A. Campos-Jiménez, J. A. Vílchez-Membrilla, C. Cobos-Sánchez, and F. J. García-Pacheco, "Analytical solutions to minimum-norm problems," *Mathematics*, vol. 10, no. 9, p. 1454, Apr. 2022.
[29] M. L. Rohan, R. T. Yamamoto, C. T. Ravichandran, K. R. Cayetano, O. G. Morales, D. P. Olson, G. Vitaliano, S. M. Paul, and B. M. Cohen, "Rapid mood-elevating effects of low field magnetic stimulation in depression," *Biol. Psychiatry*, vol. 76, no. 3, pp. 186–193, Aug. 2014.
[30] M. Shafi, A. P. Stern, and A. Pascual-Leone, "Adding low-field magnetic stimulation to noninvasive electromagnetic neuromodulatory therapies," *Biol. Psychiatry*, vol. 76, no. 3, pp. 170–171, Aug. 2014.

JOSE A. VÍLCHEZ MEMBRILLA received the B.S. degree in physics and the M.S. degree in physics, nanotechnology and radiations from the University of Granada, Spain, in 2019 and 2020, respectively. He is currently pursuing the Ph.D. degree with the Electronic Group, University of Cadiz, Spain. In 2022, he received a grant to stay as a visitor with the Department of Neuroscience and Biomedical Engineering, Aalto University, Espoo, Finland. His research is mainly focus on the design of optimal electromagnetic coils for bioengineering and electronics applications. He is a member of the Electronic Group, University of Cadiz.

MARIO F. PANTOJA (Senior Member, IEEE) received the B.S., M.S., and Ph.D. degrees in electrical engineering from the University of Granada, Granada, Spain, in 1996, 1998, and 2001, respectively. Since 2016, he has been a Full Professor at the University of Granada. He has published more than 60 refereed journal articles and book chapters, and more than 100 conference papers and technical reports, and he has participated in more than 50 national and international projects with public and private funding. His research interests include the areas of time-domain analysis of electromagnetic radiation and scattering problems, optimization methods applied to antenna design, terahertz technology, bioelectromagnetics, and nanoelectromagnetics. He was a recipient of 2002 International Union of Radio Science (URSI) Young Scientist Award. He has also received grants to stay as a Visiting Scholar at the Dipartimento Ingenieria dell'Informazione, University of Pisa, Italy, the International Research Centre for Telecommunications and Radar, Delft University of Technology, The Netherlands, and the Antenna and Electromagnetics Group, Denmark Technical University. In addition, he received 2015 Fulbright Grant to collaborate with the Computational Electromagnetics and Antenna Research Laboratory, Pennsylvania State University, USA.

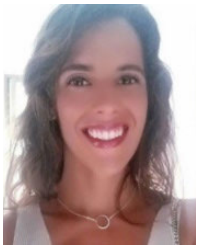

ANA P. VALERGA PUERTA holds a Ph.D. degree in materials manufacturing and environmental engineering from the University of Cadiz. Her research is focused on reverse engineering and digital fabrication with different types of materials and techniques. She is also an expert in the analysis of the behavior of materials manufactured with additive manufacturing.

VICTOR H. SOUZA graduated in medical physics in 2011, and the Ph.D. degree from the University of São Paulo, Brazil, in 2018. From 2018 to 2022, he worked as a Post-Doctoral Researcher at Aalto University, Finland, where he is currently the Director of the ConnectToBrain Laboratory and a Research Fellow. He develops instrumentation, methods, and applications for brain stimulation. He created human and preclinical multi-coil TMS devices to study network brain functions and created the first open-source neuronavigation software for TMS, named InVesalius, which is currently used in many research groups worldwide. His experimental research focuses on understanding the human motor system.

CLEMENTE COBOS SÁNCHEZ received the B.Sc. and M.Sc. degrees in physics from the Universidad de Granada, Spain, and the Ph.D. degree from the Sir Peter Mansfield Imaging Centre, University of Nottingham, U.K., in 2008. He has been a Senior Lecturer with the Department of Electronics, Universidad de Cádiz, Spain, since 2018. His research focuses on developing improved equipment and techniques for transcranial magnetic stimulation and magnetic resonance imaging and applying them in biomedical studies. His current research interest includes deep learning through physics-constrained networks.